Superparamagnetic Behavior of the Magnetic Hysteresis Loop in the Fe₂O₃@Pt Core-Shell Nanoparticles

Z. Alborzi [1*], A. Hassanzadeh [2,3], M. M. Golzan [1,3]

1- Department of Physics, Faculty of Science, Urmia, I. R. Iran
2- Department of Chemistry, Faculty of Science, Urmia, I. R. Iran
3- Nanotechnology Research Center of Urmia University, Urmia, I. R. Iran

(*) Corresponding author: zahra_alborzi@yahoo.ca

Abstract:

Studies of the magnetization of Fe₂O₃@Pt nanoparticles at room temperature showed that there is superparamagnetic contribution with high saturation magnetization about 12.35(emu/g), and soft ferromagnetic contribution with narrow coercive field about 58(Oe). In this paper we fitted the hystersis loop of sample with Brillouin function that demonstrating existence of superparamagnetic phase. Total angular momentum quantum number J With computations performance, gave consistent value at high level that could be the reason into existence of spin clusters. Upshot theoretically, magnetic susceptibility of this sample was calculated from the Brillouin function at fields less than 1000(Oe) from 0.1 to 400 K to determine the high-temperature susceptibility.

Keywords: *α-Fe₂O₃@Pt core-shell nanoparticles, Magnetization, Superparamagnetic, Brillouin function, Susceptibility.*

1. INTRODUCTION

The platinum-hematite Fe₂O₃@Pt core-shell nanoparticles have attracted significant attention because of its complex magnetic properties and its usage in industry and medicine applications such as drug-targeting, cancer therapy, lymph node imaging or hyperthermia. There are other applications of magnetic nanoparticles, e.g. in ferrofluids, high performance permanent magnets, high-frequency electronics and magnetic refrigerators [1-3]. Core-shell nanoparticles were generally synthesized through two synthetic ways: precipitation, surface reaction and controlled deposition using preformed primary particles.

Recently in year 2010, Chen and co-workers synthesized the α-Fe₂O₃@Pt urchin-like composites (fewer than 10 nanometers) and investigated their magnetic and electrocatalytic properties. They have

seen superparamagnetic phase in this sample [4]. The descriptions of intricate behavior of magnetic materials subjected to magnetic fields under non-equilibrium thermodynamic conditions have gained a renewed interest in recent years [5]. Although the magnetism of fine particles has been studied for many years, there is the rich variety of phenomena which remain to be understood and explained. The adequate description of the whole magnetization curve is more difficult. In recent years many researchers work in this field work [6-9]. Very small magnetic particles exhibit a gradual transition to paramagnetism. For sufficiently small numbers N of atoms, the interatomic exchange ensures that the spins are all parallel, so that the particle behaves like a superparamagnetic single spin or macrospin of length N. Nanoparticles containing hundreds or thousands of atoms are intermediate between the superparamagnetic small clusters and

true ferromagnets. Very small particles have a low coercivity due to superparamagnetic excitations [10]. As outlined by Bean and Livingston (1959), superparamagnetism involves two phenomena: the Langevin-type alignment of macrospins in an external field and the superparamagnetic blocking or freezing of the magnetization reversal [11].

Moreover, in magnetic materials, approximation of magnetization was performed by the Brillouin function that measured in applied magnetic field along the easy axis. The accuracy of these approximations in a wider region of magnetization is not high.

In the present work, we will try to find an approximation based on the Brillouin equation satisfying the following necessity:

1. It should be consistent with the phenomenological description of magnetization.
2. The used component of theoretical formula should be fitted with the experimental data of samples.
3. It achieves high accuracy in the whole region of magnetization.

For this purposes, we utilized the magnetic experimental data of Fe_2O_3@Pt core-shell nanoparticles that their magnetization results were measured by vibrating sample magnetization (VSM). The experimental data was well fitted to equation (1-3.2) (approximately, the square chi coefficient is 10^{-6}), which means that the Fe_2O_3@Pt core-shell NPs are essentially superparamagnetic nanoparticles. Ultimately, in sight of theory, magnetic susceptibility of samples was calculated and by this computation, good result was given.

2. MATERIALS AND METHODS

2.1. Synthesis of α-Fe_2o_3@Pt core-shell NPs

α-Fe_2o_3@Pt core-shell NPs were synthesized by chemical reduction of Pt onto the Fe_2o_3 core. The process was as followed: 140 mL of Fe_2O_3 (Merck; 10^{-3} M) aqueous solution was placed in ultrasonic bath for 50 min. Then 7 mL of tri-sodium citrate dihydrate (Merck; 1×10^{-1} M) was added to Fe_2O_3 solution and were violently stirred for 15 min. When the mixture was stirred and heated to 80 °C, 1 mL

of K_2PtCl_6 (Merck; 2×10^{-2} M) was added and finally 7.5 mL of $NaBH_4$ (Merck; 1.32 M) was added under stirring for 30 min at 40 °C, until a brown-blackish colloidal solution was formed(See Figure 1). Pt shells were formed by reduction of Pt^{4+} onto the Fe_2O_3-core nanoparticles surfaces using tri-sodium citrate dihydrate as both a reductant and a stabilizer material.

Figure 1: Solution of Fe_2O_3 (Left hand-side) and Fe_2O_3@Pt core-shell NPs (Right hand-side)

3. RESULTS AND DISCUSSION

3.1. TEM studies

Transmission electron microscopy (TEM) was employed for particles size measurement, shape evaluation and core-shell formation confirmation. TEM confirms Fe_2O_3@Pt core-shell NPs formation and it is clearly shown that the shape of NPs is nearly spherical and has an average diameter of 25 nm (See Figure 2). Besides, it shows that the dark magnetite particles are individually coated with a uniform platinum shell with a thickness of ca. 3 nm.

3.2. VSM measurements

Vibrating sample magnetometer (VSM) with a sensitivity of 10^{-3} emu and magnetic field up to 10 kOe was utilized to evaluate the magnetic saturation and hysteresis loops of NPs at room temperature
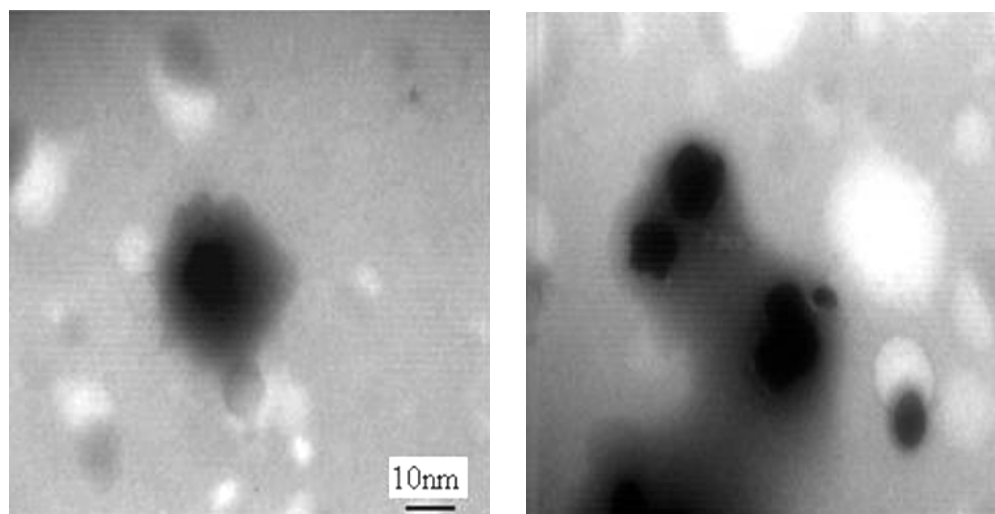
Alborzi, *et al.*

Figure 2: TEM images of Fe$_2$O$_3$@Pt core-shells.
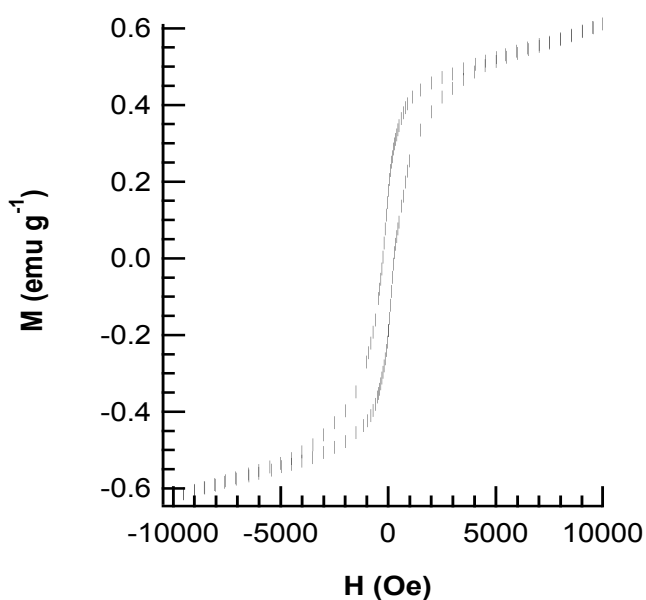

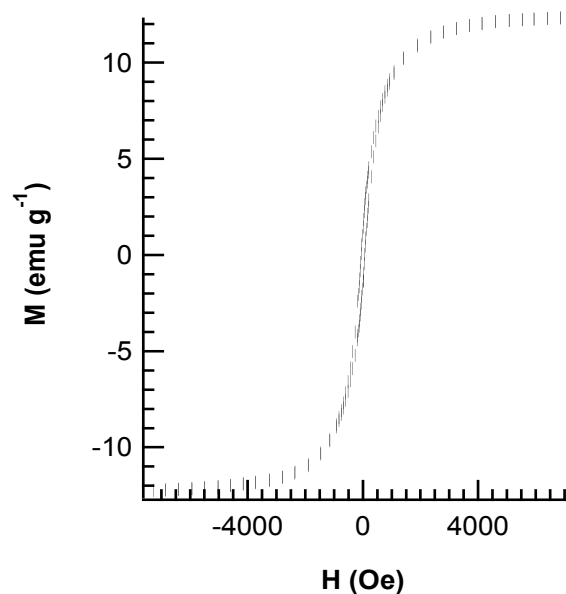*Figure 3: VSM result for Fe$_2$O$_3$@Pt core-shell NPs at room temperature*

Figure 4: VSM result for Fe$_2$O$_3$ (Merck) as reference sample

with field sweeping from -10 to +10 kOe. It is worth noting that the Fe$_2$O$_3$ (Merck) was considered as a reference sample and it was compared with Fe$_2$O$_3$@ Pt core-shell NPs to gain some of the results. Hysteresis loop of magnetization of samples were shown in Figure 3 and Figure 4.

This phenomenon is known as magnetic hysteresis. Key parameters of the hysteresis loop are the coercivity *H*c, at which the magnetization is zero, and the remanent magnetization or remanence M$_r$.

Coercivity and remanence are complemented by parameters describing the loop shape and the area under the loop [10]. The magnetic results of these samples were observed in Table 1.

Attention to the magnetic measurements, the coefficient of squareness of hysteresis loops is K$_P$ that equals to $\frac{M_r}{M_s}$, where M_r is a remanent magnetization, M_s is a saturation magnetization. These results were in Table 1. The measured

Sample	Mr (emu/g)	Ms (emu/g)	Hc⁻ (Oe)	Hc⁺ (Oe)	Loop area (Oe)×(emu/g)	K_P (Dimensionless)
Fe_2O_3(Merck)	0.177	0.548	-260	289	979.2	0.322
Fe_2O_3@Pt core-shell	1.429	12.129	-57.8	62.8	2150.2	0.139

hysteresis loop of Fe_2O_3(Merck) show that this sample approximately is in hard ferromagnetic materials group and the measured hysteresis loop of Fe_2O_3@Pt core-shell NPs show that behavior of this sample is in weak ferromagnetic phase, which can be categorized in soft magnetic materials group [12] (See Figure 3-5 & Table 1).

We have assumed that the magnetic dipole moment can take all possible orientations with respect to the applied magnetic field, whereas in reality it can have only discrete orientations because of spatial quantization. If we incorporate the quantization into the derivation of the total magnetization, we obtain:

$$M(H,T) = NJg\,\mu_\beta F(J,y) \qquad (1)$$

$$F(J,y) = (1+\frac{1}{2J})\coth[(1+\frac{1}{2J})y] - \frac{1}{2J}\coth[\frac{y}{2J}]$$

$$(2)$$

$$y = \frac{Jg\,\mu_\beta H}{K_B(T-\theta_P)} \qquad (3)$$

Where N is the number of atoms per unit of gram, J is the total angular momentum quantum number, g is the lande-g value approximately is equal to 2.01; μ_β is the Bohr-Magneton moment, $F(J,y)$ is the Brillouin function, T is the ambient temperature and θ_P is the Curie temperature. Which (2) equation is equal to the Langevin function in the limit that $J \to \infty$ [13].

By allowing the values for N, J and θ_P to float, we fitted the experimental data with the equation (1). As you can see in Figure 5, we have one of the best fitted experimental results with theory.

After fitting, the value of total angular momentum quantum number J was equal to ≈ 8000, that this can be another reason for the formation of clusters in sample. The Curie temperature calculated for the sample was 0.02 K and $N \approx 10^{16}$ (gr⁻¹).

With decreasing the size of Fe_2O_3 particles in during of synthesis, the amount of coercivity was decreased. It seems that atoms of Fe_2O_3 behave in the ferromagnetic phase and existence of Pt shell on (Fe_2O_3) core can have the most shares in high saturation magnetization. High magnetization of this sample, can be the evidence of formation of clusters in sample. In addition, the saturation magnetization will be increased by decreasing particles size [14].

Based on magnetic measurement (See Table 1), the squareness K_P of the Fe_2O_3@Pt core-shell NPs is less than that of Fe_2O_3 (Merck), this means that initial phase of Fe_2O_3, after coating the Pt shell, converts to the superparamagnetic phase. When the magnetic cluster size decreases its magnetic energy drops and approximates to the energy of heat movement that causes an enhancement of the superparamagnetic contribution into magnetization. As the experimental data are well fitted to the Brillouin function, it seems that the Fe_2O_3@Pt core-shell NPs are essentially superparamagnetic nanoparticles.

3.3. Theoretical susceptibility

The properties of a material are defined not only by the magnetization, or the magnetic induction, but also by the way in which these quantities vary with the applied magnetic field. The ratio of M to H is called the susceptibility:

$$\chi = \frac{M(H,T)}{H} \qquad (4)$$

$$\chi = \frac{NJg\,\mu_\beta F(J,y)}{H} \qquad (5)$$

Susceptibility function has two variables: H (magnetic field) and T (temperature). Susceptibility function at room temperature could be plotted by the experimental data of magnetization of sample at room temperature (See Figure 6).

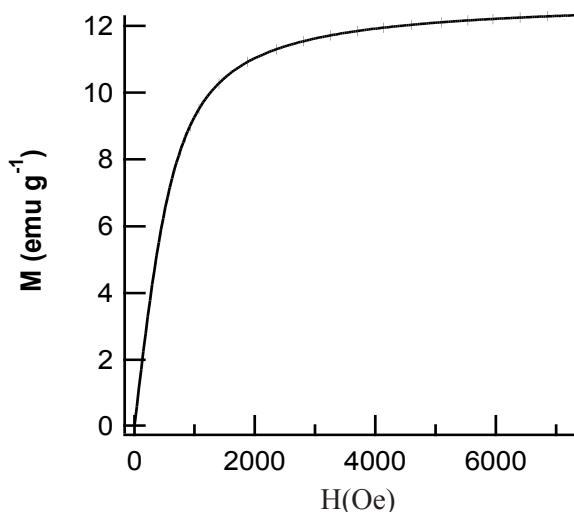At room temperature, the maximum value of susceptibility occurs at field 282.2(Oe).

Alborzi, *et al.*

Figure 5: *The superparamagnetic contribution to the magnetization of the Fe$_2$O$_3$@Pt core-shell NPs at room temperature. The experimental data (dots) have the best fits (solid lines) with the theoretical curves.*
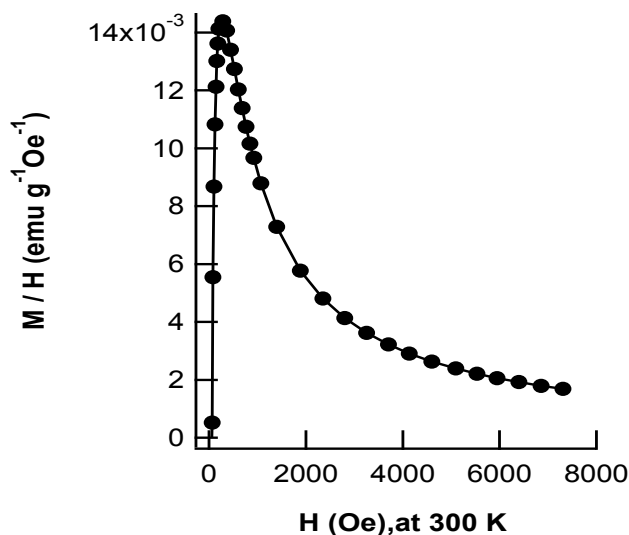

Figure 7: *The magnetic susceptibility of sample, ● line at 40.2(Oe), ■ line at -57.2(Oe) , ▼ line at field 282.2(Oe) and ▲ line at field 842.2(Oe).*

Figure 6: *The magnetic susceptibility ($\frac{M(H,T)}{H}$) of sample at room temperature.*

Figure 8: *Magnetic susceptibility of sample at field -57.2(Oe).The experimental data (dots) has the approximate best fits (solid lines) with the theoretical curves.*

Superconducting quantum interference device (or SQUID) is a device which is capable of measuring susceptibility of samples. In this device magnetic field was stabled for example in 100(Oe). Then susceptibility of sample was given with change of temperature.

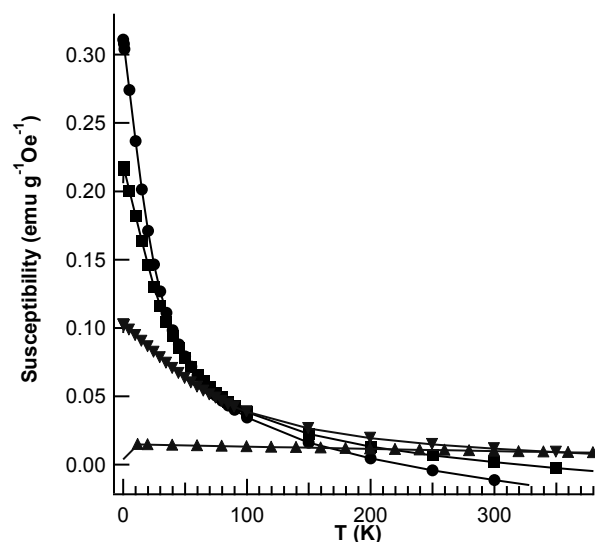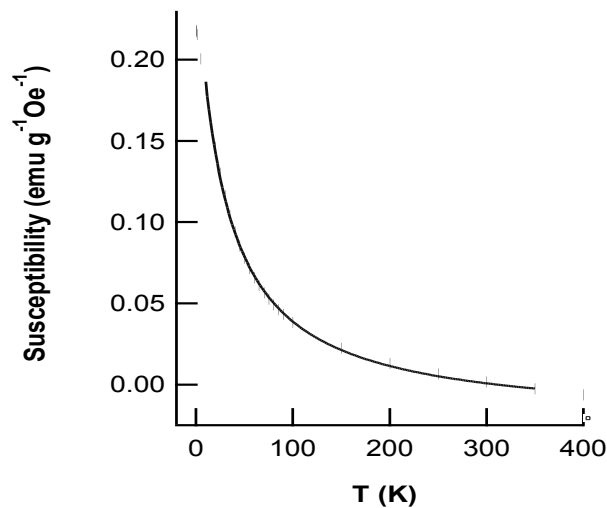After fitting the experimental data of magnetization of sample with equation (1-3.1), we reach the function of $M(H,T)$. Theoretically, without use of SQUID device, the susceptibility of sample was plotted at fields less than 1000(Oe) from 0.1 to 400 K (See Figure 7).

It was indicated in Figure 7 that with increasing the magnetic field for measuring of susceptibility, maximum value of susceptibility is increased. Also with decreasing the magnetic field, graph of

susceptibility at high temperatures was entered to the negative zone of susceptibility. It seems that diamagnetism's contribution of susceptibility is appearing.

Above their Curie temperatures, θ_p, ferromagnetic materials become paramagnetic, and their susceptibilities follow the Curie-Weiss law, with a value of θ approximately equal to θ_P [13]

$$\chi = \frac{C}{T - \theta} + \chi_{dia} \tag{6}$$

By fitting one of the graphs of susceptibility, it could be shown that this behavior is correct (See Figure 8). Furthermore, the diamagnetism's susceptibility contribution was observed on sample after fitting. The value of χ_{dia} was obtained -0.02(emu/ (g.Oe)).

4. CONCLUSION

In brief, we found a new way to the synthesis of α-Fe$_2$O$_3$@Pt core-shell nanoparticles to use as the drug-targeting, cancer therapy and etc. Based on magnetic measurement, as the experimental data are well fitted to the Brillouin function, it seems that the α-Fe$_2$O$_3$@ Pt core-shell NPs are essentially superparamagnetic nanoparticles that with the calculation performed, its total angular momentum quantum number J has became 8000. The high magnetization and high total angular momentum quantum number J could be a reason of the presence of spin clusters in sample. Theoretically, without use of SQUID device, the susceptibility of sample at fields less than 1000(Oe) was plotted from 0.1 to 400 K. Susceptibility of sample follows the Curie-Weiss law.

REFERENCES

1. C. C. Berry, A. S. G. Curtis, Functionalisation of magnetic nanoparticles for applications in biomedicine, J. Phys. D: Appl. Phys. Vol. 36, (2003), pp. 198–206.

2. P. Tartaj, M. P. Morales, S. V. Verdaguer, T. G. Carreno, C. J. Serna, The preparation of magnetic nanoparticles for applications in biomedicine, J. Phys. D: Appl. Phys. Vol. 36, (2003), pp. 182–197.

3. J. A. Nelson, L. H. Bennett, M. J. Wagner, Solution Synthesis of Gadolinium Nanoparticles, J. AM. CHEM. SOC. Vol. 9, (2002), pp. 2979-2983.

4. Y. Chen, K. Zhang, Y. Min, Y. Zhang, R. Zhang, Facile route to synthesis α-Fe2O3/ Pt urchin-like composites and their magnetic and electrocatalytic properties, material chemistry and physics. Vol. 123, (2010), pp. 378-384.

5. K. Chwastek, Modelling magnetic properties of MnZn ferrites with the modified Jiles–Atherton description, J. Phys. D: Appl. Phys. Vol. 43, (2010), pp. 15005-15010.

6. M. M. Golzan, D. R. Mckenzie, D. J. Miller, S. J. Collocott, G. A. J. Amaratunga, Magnetic and spin properties of tetrahedral amorphous carbon, Diamond and related materials, Vol. 4, (1995), pp. 912-916.

7. N. Dave, B. G. Pautler, S. S. Farvid, P. V. Radovanovic1, Synthesis and surface control of colloidal Cr^{3+}-doped SnO$_2$ transparent magnetic semiconductor nanocrystals, Nanotechnology. Vol. 21, (2010), pp. 134023-134030.

8. D. Ortega, E. Velez-Fort, D. A. Garcia, R. Garcia, R. Litran, C. Barrera, A. Solano, M. Ramirez-Del-Solar, M. Dominguez, Size and surface effects in the magnetic properties of maghemite and magnetite coated nanoparticles, Phil. Trans. R. Soc. A. Vol. 368, (2010), pp. 4407–4418.

9. H. Liu, J. Wu, J. H. Min, P. Hou, A. Y. Song, Y. K. Kim, Non-aqueous synthesis of water-dispersible Fe$_3$O$_4$– Ca$_3$(PO$_4$)$_2$ core–shell nanoparticles, Nanotechnology. Vol. 22, (2011), pp. 055701-055708.

10. R. Skomski, Simple Models of Magnetism, Oxford University Press, New York, Vol. 228, (2008), p. 3.

11. C. P. Bean, J. D. Livingstone, Superparamagnetism, J. Appl. Phys. Vol. 30, (1959), pp. 120-129.

12. A. H. Morrish, The physical principles of Magnetism, John WILEY & Sons, Ins. New York, Vol. 483, (1965), pp. 3-5.

13. N. A. Spaldin, Magnetic materials: fundamentals and device applications, Cambridge, United Kingdom, (2003), p. 46.

14. I. V. Vasylenkoa, K. S. Gavrylenkoa, V. G. Il'yin, V. Golubc, G. Goloverda, V Kolesnichenko, A. W. Addisond, V. V. Pavlishchuka, The metamorphosis of heterometallic trinuclear antiferromagnetic complexes into nano-sized superparamagnetic spinels, Mater. Chem. Phys. Vol. 121, (2010), pp. 47–52.